YMTHE, Volume *25*

Supplemental Information

Cholesterol-Lowering Gene Therapy Counteracts the Development of Non-ischemic Cardiomyopathy in Mice

Ilayaraja Muthuramu, Ruhul Amin, Andrey Postnov, Mudit Mishra, Joseph Pierre Aboumsallem, Tom Dresselaers, Uwe Himmelreich, Paul P. Van Veldhoven, Olivier Gheysens, Frank Jacobs, and Bart De Geest

SUPPLEMENTAL FIGURES

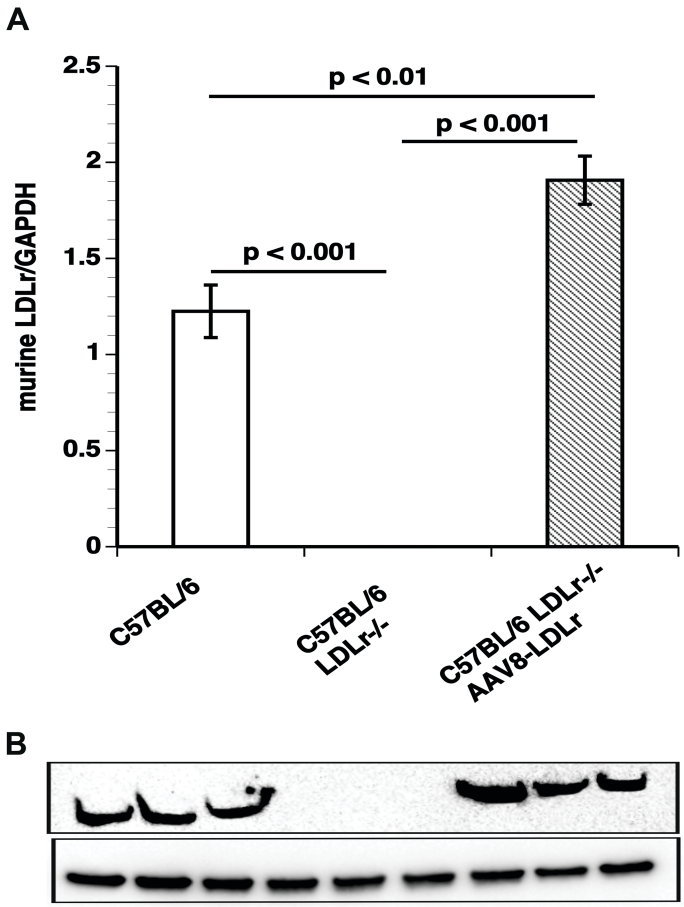

Figure S1. Murine LDLr expression in the liver. Bar graph (A) illustrating murine LDLr protein levels quantified by western blot in the liver of C57BL/6 mice (n=6), of C57BL/6 LDLr$^{-/-}$ mice (n=6), and of C57BL/6 LDLr$^{-/-}$ mice (n=6) 10 weeks after gene transfer with 2 x 10^{12} genome copies/kg of AAV8-LDLr. All protein levels were normalized to the glyceraldehyde-3-phosphate dehydrogenase (GAPDH) protein level. Representative images of western blots are shown in panel B. The first three lanes correspond to C57BL/6 mice, the next three lanes illustrate C57BL/6 LDLr$^{-/-}$ mice, and the final three lanes correspond to AAV8-LDLr-treated C57BL/6 LDLr$^{-/-}$ mice. Error bars represent SEM.

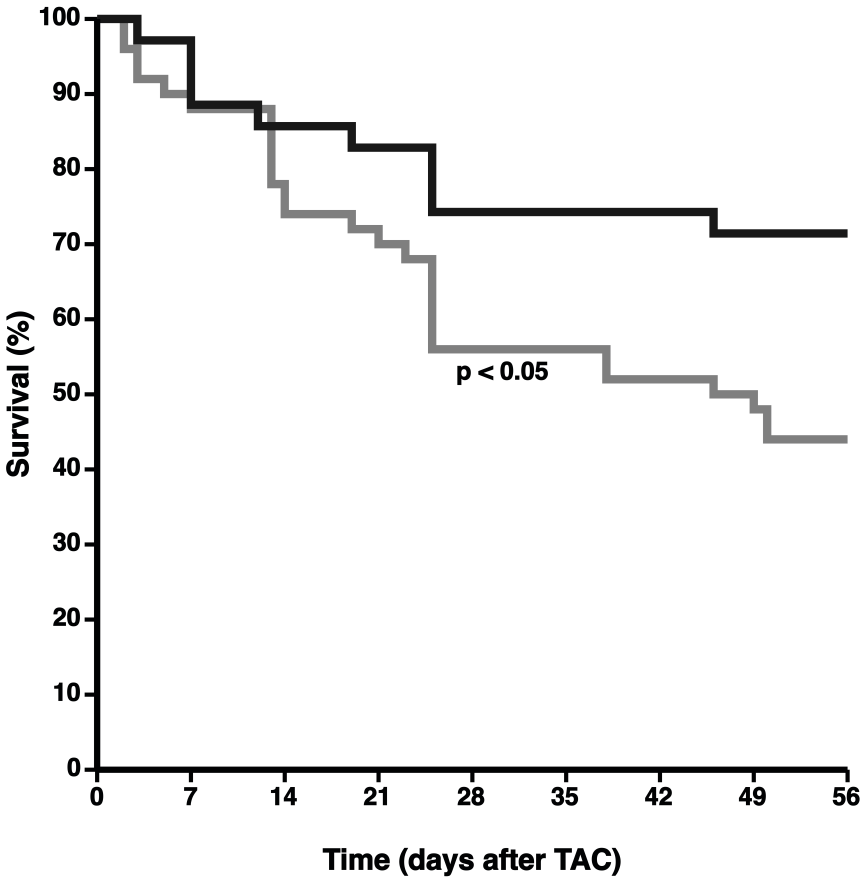

Figure S2. Comparison of Kaplan-Meier survival curves during an 8 weeks follow-up period after TAC. Control TAC mice (grey line) and AAV8-LDLr TAC mice (black line) are compared. The 0 day time-point corresponds to the induction of TAC at the age of 17 weeks. Survival analysis was performed by log-rank test.

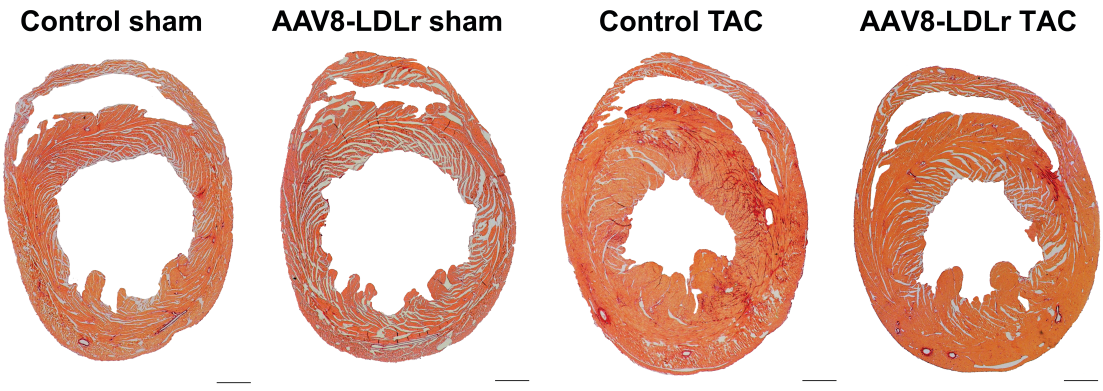

Figure S3. Representative Sirius red stained cross-sections of sham hearts and TAC hearts at day 56 after operation. Scale bar represents 1 mm.

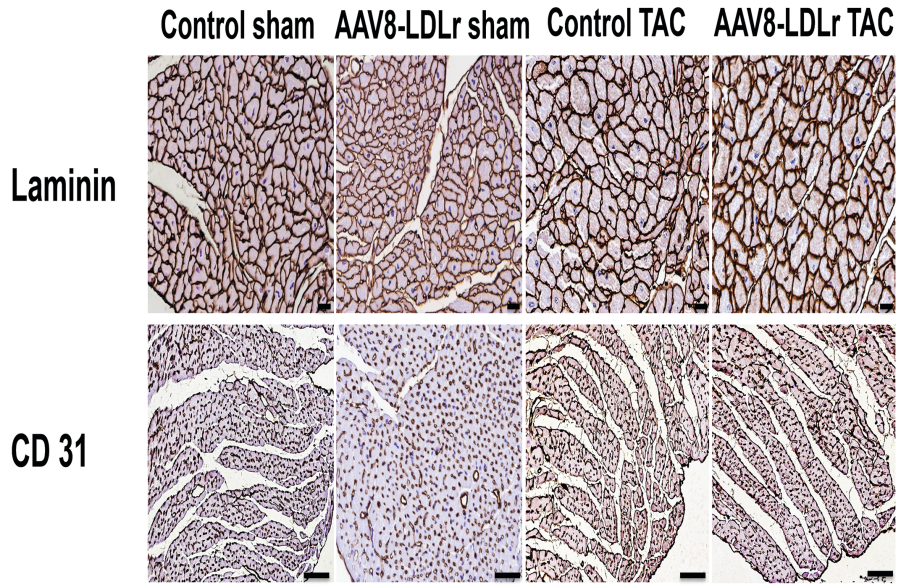

Figure S4. Immunohistochemical analysis of the myocardium of sham mice and TAC mice at day 56 after operation. Representative photomicrographs show laminin-stained cardiomyocytes and CD31-positive capillaries. Scale bar represents 50 μm.

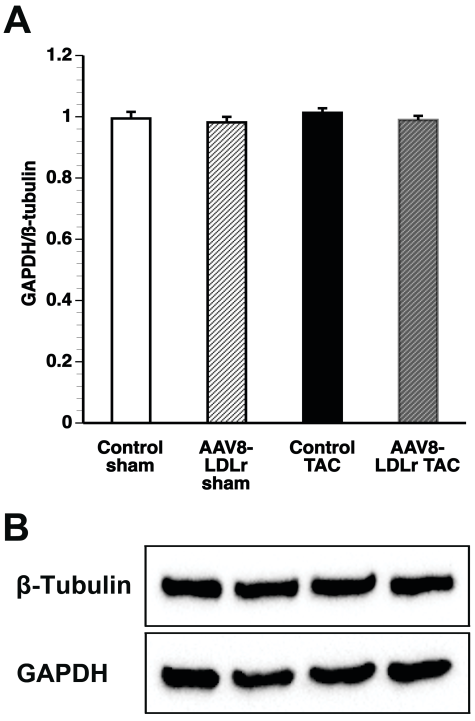

Figure S5. GAPDH is an adequate reference for normalizing protein expression levels. Bar graph (A) illustrating the GAPDH/ß-tubulin protein level ratio in the myocardium of control sham (n=10), AAV8-LDLr sham (n=10), control TAC (n=9), and AAV8-LDLr TAC (n=10) mice 8 weeks after operation. Representative images of western blots are shown in panel B. Error bars represent SEM.

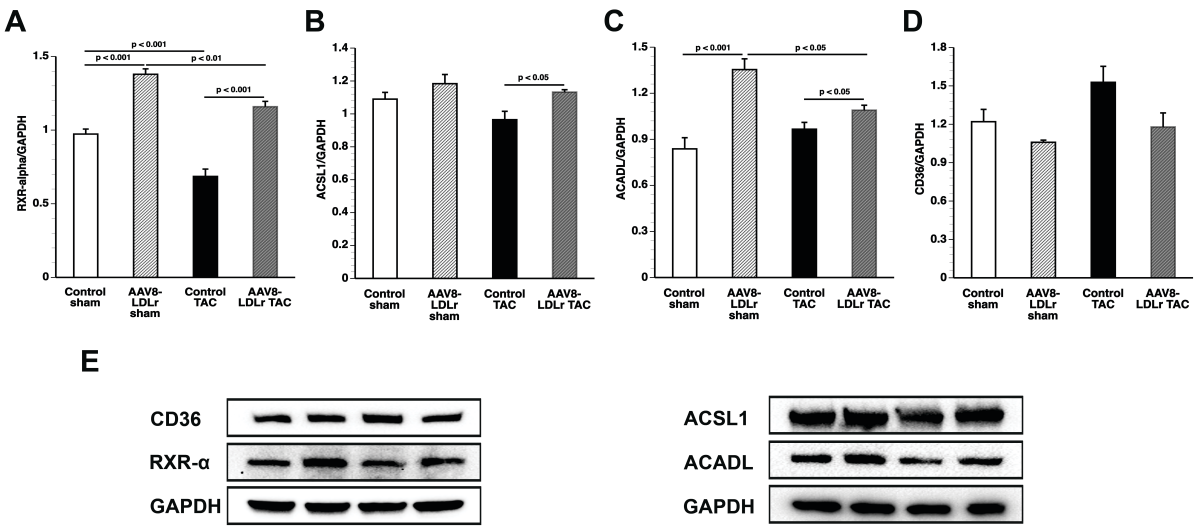

Figure S6. Quantification of RXR-α and of metabolic proteins by western blot. Bar graphs illustrating RXR-α (A), ACSL1 (B), ACADL (C), and CD36 (D) protein levels quantified by western blot in the myocardium of control sham (n=10), AAV8-LDLr sham (n=10), control TAC (n=9), and AAV8-LDLr TAC (n=10) mice 8 weeks after operation. All protein levels were normalized to the GAPDH protein level. Representative images of western blots are shown in panel E. Error bars represent SEM.

SUPPLEMENTAL TABLES

Table S1. Total and non-HDL, VLDL, IDL, LDL and HDL plasma cholesterol (mmol/L) at day 10 after gene transfer with 2 x 10^{12} genome copies/kg of AAV8-LDLr in female C57BL/6 LDLr$^{-/-}$ mice compared to control female C57BL/6 LDLr$^{-/-}$ mice.

	Controls	AAV8-LDLr
Total	9.26 ± 0.39	1.59 ± 0.08****
Non-HDL	7.89 ± 0.36	0.714 ± 0.039****
VLDL	1.75 ± 0.10	0.160 ± 0.010****
IDL	3.57 ± 0.31	0.235 ± 0.013****
LDL	2.57 ± 0.12	0.318 ± 0.018****
HDL	1.37 ± 0.07	0.879 ± 0.054***

Data are expressed as means ± S.E.M. (n=6 for each condition). Lipoproteins were isolated by ultracentrifugation. ***: $p<0.001$; ****: $p<0.0001$ for comparison versus controls.

Table S2. Myocardial lipid levels 8 weeks after sham operation or after TAC.

	Control sham	AAV8-LDLr sham	Control TAC	AAV8-LDLr TAC
Number of mice	10	10	9	11
Phospholipids (nmol/mg tissue)	51.6 ± 0.9	52.0 ± 1.2	45.9 ± 0.9§§	48.2 ± 1.1
Cholesterol (pmol/nmol phospholipids)	75.4 ± 1.7	73.7 ± 2.4	82.5 ± 3.9	77.0 ± 3.7
Cholesteryl esters (pmol/nmol phospholipids)	16.3 ± 2.4	8.79 ± 3.11°	20.6 ± 5.6	4.87 ± 0.56**
Triglycerides (pmol/nmol phospholipids)	68.4 ± 4.9	52.8 ± 3.6°	43.4 ± 2.3§§	56.9 ± 6.8
Free fatty acids (pmol/nmol phospholipids)	4.45 ± 1.53	12.4 ± 4.3	11.5 ± 1.5§	11.8 ± 1.8
Sphingomyelin (pmol/nmol phospholipids)	24.9 ± 2.0	27.3 ± 3.6	34.3 ± 1.9§	32.5 ± 2.2

Sham operation or TAC was performed at the age of 17 weeks.
Data are expressed as means ± SEM. °: $p<0.05$ versus control sham. §: $p<0.05$; §§**:** $p<0.01$ versus respective sham groups.**: $p<0.01$ versus control TAC.

Table S3. Morphometric and histological parameters of the left ventricular myocardium 8 weeks after sham operation and after TAC in C57BL/6 LDLr$^{-/-}$ mice.

Sham operation or TAC was performed at the age of 17 weeks.

	Control sham	AAV8-LDLr sham	Control TAC	AAV8-LDLr TAC
Number of mice	15	22	23	23
LV wall area (mm^2)	9.06 ± 0.17	8.67 ± 0.17	12.4 ± 0.4§§§	10.6 ± 0.4§§§***
Septal wall thickness (µm)	1070 ± 14	1060 ± 20	1320 ± 40§§§	1230 ± 30§§
Anterior wall thickness (µm)	1100 ± 10	1120 ± 20	1370 ± 30§§§	1300 ± 40§
Cardiomyocyte cross-sectional (μm^2)	230 ± 17	187 ± 6$^{°}$	480 ± 20§§§	410 ± 20§§§*
Cardiomyocyte density (number/mm^2)	4520 ± 280	5630 ± 170$^{°°°}$	3050 ± 120§§§	3480 ± 170§§§
Capillary density (number/mm^2)	6040 ± 340	7310 ± 220$^{°}$	4480 ± 240§§§	4360 ± 170§§§
Relative vascularity (μm^{-2})	0.00617 ± 0.00041	0.00716 ± 0.00027$^{°}$	0.00315 ± 0.00016§§§	0.00319 ± 0.00013§§§

Data are expressed as means ± SEM. °: p<0.05;°°°: p<0.001 versus control sham. §: p<0.05; §§: p<0.01; §§§: p<0.001 versus respective sham groups. *: p<0.05; ***: p<0.001 versus control TAC.

Table S4. Quantification of glucose uptake in the myocardium determined by micro-PET parameters 8 weeks after sham operation or after TAC in C57BL/6 LDLr$^{-/-}$ mice.

	Control sham	AAV8-LDLr sham	Control TAC	AAV8-LDLr TAC
Number of mice	10	10	11	11
Maximal SUV	9.75 ± 1.58	9.69 ± 1.80	20.7 ± 1.0§§§	14.6 ± 1.6§*
SUV 50%	6.99 ± 1.17	6.89 ± 1.32	13.9 ± 0.8§§§	10.0 ± 1.1§§*
Volume 50% (mm^3)	103 ± 7	96.5 ± 3.1	143 ± 17§	97.8 ± 5.5**
SUV 75%	8.25 ± 1.35	8.16 ± 1.53	17.2 ± 0.9§§§	12.2 ± 1.3§*
Volume 75% (mm^3)	40.5 ± 3.0	35.1 ± 2.4	36.4 ± 6.0	29.3 ± 3.6
Total myocardial uptake (%)	4.90 ± 0.96	4.29 ± 0.96	17.9 ± 2.4§§§	7.84 ± 1.16§*
SUV left quadriceps	0.375 ± 0.054	0.381 ± 0.045	0.318 ± 0.056	0.402 ± 0.067

Sham operation or TAC was performed at the age of 17 weeks. Micro-PET analysis was performed at the age of 25 weeks.
SUV: standardized uptake value. SUV 50%: average SUV in voxels with a value above 50% of the maximal SUV. SUV 75%: average SUV in voxels with a value above 75% of the maximal SUV.
Volume 50%: integrated volume of voxels with a value above 50% of the maximal SUV. Volume 75%: integrated volume of voxels with a value above 75% of the maximal SUV.
Data are expressed as means ± SEM. §: $p<0.05$; §§§: $p<0.001$ versus respective Sham groups; *: $p<0.05$; **: $p<0.01$ versus Control TAC.

SUPPLEMENTAL MATERIALS AND METHODS

Construction, generation, and production of gene transfer vectors-Cholesterol lowering gene therapy was performed using an AAV8 vector containing a hepatocyte-specific expression cassette to induce expression of the murine low-density lipoprotein receptor (LDLr) (AAV8-LDLr). The expression cassette of this vector consists of the 1272 bp *DC172* promoter, comprising an 890 bp α_1*-antitrypsin* promoter fused together with 2 copies of the 160 bp α_1*-microglobulin* enhancer[1], upstream of the human *A-I 5'UTR* containing the first intron (247 bp) followed by the murine *LDLr* cDNA sequence (2598 bp), and the rabbit ß-globin polyadenylation signal (127 bp). The transcriptional regulatory sequences in this expression cassette are hepatocyte-specific[1]. AAV vector production was performed as described[2].

In vivo experiments on the effect of cholesterol lowering gene therapy on cardiac remodeling-All experimental procedures in animals were performed in accordance with protocols approved by the Institutional Animal Care and Research Advisory Committee of the Catholic University of Leuven (Approval number: P154/2013). At the age of 12 weeks, female C57BL/6 LDLr$^{-/-}$ mice, originally purchased from Jackson Laboratories (Bar Harbor, ME, USA), were fed standard chow diet (Sniff Spezialdiäten GMBH, Soest, Germany) supplemented with 0.2% cholesterol 10% coconut oil to induce pronounced hypercholesterolemia. Gene transfer in C57BL/6 LDLr$^{-/-}$ mice was performed at the age of 15 weeks by tail vein injection of 2 x 10^{12} genome copies/kg of AAV8-LDLr. Control mice were untreated. To induce pressure overload, TAC was performed two weeks later[3, 4]. Briefly, anesthesia was performed with a single intraperitoneal injection of sodium pentobarbital (Nembutal®, Ceva Sante Animale, Brussels, Belgium) at a dose of 40-70 mg/kg. Mice were put in supine position and temperature was maintained at 37°C with a heating pad. A horizontal skin incision of 0.5 cm to 1 cm in length was made at the level of the suprasternal notch. A 2 mm to 3 mm longitudinal cut was performed in the proximal portion of the sternum and the thymus gland was retracted. This allowed visualization of the aortic arch under low-power magnification. A wire with a snare at the end was passed under the aorta between the origin of the right innominate artery and the left common carotid artery. A 7-0 silk suture (Ethicon, Johnson & Johnson, Livingston, Scotland) was snared with the wire and pulled back around the aorta. Subsequently, a bent 27-gauge needle (BD Microlance®, BD, Franklin Lakes, New Jersey) was placed next to the aortic arch and the suture was snugly tied around the needle and the aorta. Afterwards, the needle was quickly removed. The skin was closed and mice were allowed to recover on a warming pad until they were fully awake. The sham procedure was identical except that no constriction on the aorta was applied.

In vivo hemodynamic measurements-Invasive hemodynamic measurements were performed 8 weeks after TAC or after sham operation. Mice were anesthetized by intraperitoneal administration of 1.4 g/kg urethane (Sigma, Steinheim, Germany). Body temperature was maintained with a heating pad and monitored with a rectal probe. An incision in the right carotid artery was made with a 26-gauge needle between a distal and proximal non-occlusive ligation of the artery. A 1.0 French Millar pressure catheter (SPR-67/NR; Millar instruments, Houston, Texas, USA) was inserted and advanced to the left ventricle (LV). After stabilisation of the catheter, heart rate, maximal systolic LV pressure, minimal diastolic LV pressure, the peak rate of isovolumetric LV contraction (dP/dt_{max}), and the peak rate of isovolumetric LV relaxation (dP/dt_{min}) were measured. The end-diastolic LV pressure was calculated manually from the pressure in function of time curves. The time constant of isovolumetric LV pressure fall (tau) was calculated using the method of Weiss *et al.*[5]. Arterial blood pressure measurements were obtained after withdrawal of the catheter from the LV to the ascending aorta. Data were registered with Powerlab Bridge Amplifier and Chart Software (sampling rate 2000 Hz; ADInstruments Ltd, Oxford, United Kingdom).

Blood sampling-Blood was collected by puncture of the retro-orbital plexus. Anticoagulation was performed with 0.1 volume of 4% trisodium citrate and plasma was immediately isolated by centrifugation at 1100 g for 10 min and stored at -20°C.

Plasma lipoprotein analysis-Mouse lipoproteins were separated by density gradient ultracentrifugation in a swing-out rotor as described before[6]. Fractions were stored at -20°C until analysis. Non-HDL cholesterol was determined as the sum of cholesterol within very low-density lipoproteins (VLDL) ($0.95 < d < 1.006$ g/ml), intermediate-density lipoproteins (IDL) ($1.006 < d < 1.019$ g/ml), and low-density lipoproteins (LDL) ($1.019 < d < 1.05$ g/ml) lipoprotein fractions. The cut-off value (d=1.05 g/ml) between LDL and high-density lipoproteins (HDL) for murine samples was chosen based on previous work by Camus, Chapman *et al.*[7]. Cholesterol in plasma and lipoprotein fractions was determined with commercially available enzymes (Roche Diagnostics, Basel, Switzerland). Precipath L (Roche Diagnostics) was used as a standard.

Analysis of lipid peroxidation in plasma-Measurement of Thiobarbituric Acid Reactive Substances (TBARS) used for quantification of lipid peroxidation was performed according to the instructions of the manufacturer (Cayman Chemical, Ann Arbor, MI, USA).

Myocardial lipid analysis-Major lipid classes (phospholipids, cholesterol, cholesteryl esters, triglycerides, free fatty acids and sphingomyelin) in the myocardium were analyzed in myocardial lipid extracts with classical (bio)chemical assays[8-11].

Quantification of myocardial protein levels by western blot-Myocardial tissue samples were isolated 56 days after sham operation or TAC and immediately frozen in liquid nitrogen and stored at -80°C. Tissues were placed in lysing matrix tubes (QBiogene/MP Biomedicals, Solon, OH, USA), mixed with 1 ml of protein extraction buffer containing 10 mM imidazole, 300 mM sucrose, 1 mM dithiotreitol, 1mM sodium metabisulfite, 25 mM sodium fluoride, 5 mM sodium ethylenediaminetetraacetic acid, 5 mM sodium pyrophosphate, 0.3 mM phenylmethylsulfonyl fluoride, and a protease inhibitor cocktail (Roche Diagnostics Belgium, Vilvoorde, Belgium)[12], and homogenised in the FastPrep24 instrument (MP Biomedicals). Protein concentration was quantified using the Pierce BCA Protein Assay kit (Pierce Biotechnology Inc., Rockford, IL, USA). Equal amounts of proteins were separated on 4-20 % Tris-Glycine gradient gels (Bio-Rad Laboratories N.V., Temse, Belgium) and blotted onto polyvinylidene difluoride membranes (Bio-Rad Laboratories N.V.). Membranes were incubated with primary antibodies against Akt, phospho (p)-Akt (Ser/Thr), mitogen-activated protein kinase (MAPK) kinase (MEK) 1/2, p-MEK 1/2 (Ser217/221), p38 MAPK, p-p38 MAPK (Thr180/Tyr182), mammalian or mechanistic target of rapamycin (mTOR), p-mTOR (Ser2481), acetyl-coenzyme A (acetyl-CoA) carboxylase (ACC), p-ACC (Ser79), AMP-activated protein kinase (AMPK)α, p-AMPKα (Thr172), c-Jun N-terminal kinase (JNK), also referred to as stress-activated protein kinase (SAPK)/JNK, p-JNK (Thr183/Tyr185), extracellular signal–regulated kinase (ERK) 1/2, p-ERK 1/2 (Thr202/Tyr204), Smad1, p-Smad 1/5 (Ser463/465), Smad4, GLUT 4, pyruvate dehydrogenase (PDH), pyruvate dehydrogenase kinase, transforming growth factor (TGF)-β1, fatty acid synthase (FAS), long-chain acyl-CoA synthetase, member 1 (ACSL1), ß-tubulin, glyceraldehyde 3-phosphate dehydrogenase (GAPDH) (all prior antibodies from Cell Signalling Technologies, Beverly, MA, USA), peroxisome proliferator-activated receptor (PPAR-α), carnitine palmitoyltransferase IB (CPT1B), liver X receptor (LXR)-α and LXR-ß, retinoid X receptor (RXR)-α, fatty acid translocase (CD36), and long-chain acyl-CoA dehydrogenase (ACADL) (Abcam, Cambridge, UK). Protein expression was detected with Super signal west pico chemilumninescent reagents (Thermo Scientific, Rockford, IL, USA) and quantified using Image lab TM Analyzer software (Bio-Rad laboratories N.V.). All protein levels were normalized to the GAPDH protein level.

Quantification of murine LDLr expression in the liver by western blot- Liver tissue samples were isolated and immediately frozen in liquid nitrogen and stored at -80°C. The extraction, blotting, and protein quantification procedures were identical compared to the methodology described for myocardial proteins. The primary antibody for detection of the murine LDLr was obtained from Abcam (Cambrdige, UK).

Histological and morphometric analysis-After hemodynamic analysis, mice were perfused via the abdominal aorta with phosphate-buffered saline (PBS) and hearts were arrested in diastole by $CdCl_2$ (100 µl; 0.1 mol/L), followed by perfusion fixation with 1% paraformaldehyde in phosphate buffered saline. After dissection, hearts were post-fixated overnight in 1% paraformaldehyde, embedded in paraffin, and 6 µm thick cross-sections at 130 µm spaced intervals were made extending from the apex to the basal part of the left ventricle. Left ventricle (LV) remodeling was assessed by morphometric analysis on mosaic images of Sirius red-stained heart cross-sections using Axiovision 4.6 software (Zeiss, Zaventem, Belgium). LV wall area (mm^2; including the septum), anterior wall thickness, and septal wall thickness were analyzed. All geometric measurements were computed in a blinded fashion from representative tissue sections of 4 separate regions and the average value was used to represent that animal for statistical purposes.
To measure collagen content in the interstitium, Sirius Red staining was performed as previously described by Junqueira *et al.*[13]. Sirius Red polarization microscopy on a Leica RBE microscope with KS300 software (Zeiss) was used to quantify thick tightly packed mature collagen fibers as orange-red birefringent and loosely packed less cross-linked and immature collagen fibers as yellow-green birefringent. Collagen positive area was normalized to the LV remote area and was expressed as percentage. Any perivascular fibrosis was excluded from this analysis. Perivascular fibrosis was quantified as the ratio of the fibrosis area surrounding the vessel to the total vessel area. Two mid-ventricular sections were studied per animal.
Cardiomyocyte hypertrophy was analyzed on paraffin sections stained with rabbit anti-mouse laminin (Sigma; 1/50) by measuring the cardiomyocyte cross-sectional area (μm^2) of at least 200 randomly selected cardiomyocytes in the LV myocardium. Capillary density in the myocardium was determined on CD31 stained sections using rat anti-mouse CD31 antibodies (BD; 1/500). Relative vascularity in the myocardium was

determined as [(capillary density (number/mm^2)/cardiomyocyte density (number/mm^2))/cardiomyocyte cross-sectional area (μm^2)][14]. Two mid-ventricular cross-sections were analyzed per mouse.
Immunostaining for 3-nitrotyrosine was performed with rabbit anti-nitrotyrosine antibodies (Merck Millipore, Overijse, Belgium; dilution 1/250).
Apoptosis was quantified on deparaffinized tissue sections using SignalStain® cleaved caspase-3 IHC detection kit (Cell Signaling Technologies, Beverly, MA), which utilizes a polyclonal rabbit antibody to the neoepitope peptide at the end of cleaved caspase-3[15].

Evaluation of cardiac glucose metabolism by micro-positron emission tomography (micro-PET)-Glucose uptake in the myocardium and in the skeletal muscle was quantified by micro-PET using [^{18}F]-fluorodeoxyglucose (FDG) as a tracer (309 ± 22 µCi). Imaging was performed 60 min after tracer administration. Animals were anesthetized by inhalation of 2% isoflurane in 100% oxygen and underwent static imaging for 10 minutes on a micro-PET Focus 220 scanner (Concorde Microsystems, Knoxville, TN, USA). Images were reconstructed with ordered subset expectation maximization algorithm with 6 iterations (OSEM3D 6i) and analyzed with PMOD v.3.4 (Pmod Technologies, Zurich, Switzerland). To exclude any effect of diurnal variability, micro-PET data acquisition was consistently performed within the same 2 hours' time frame of the day. The simultaneous quantification of skeletal SUVs was performed since myocardial glucose metabolism is not always parallel to skeletal and whole-body glucose metabolism[16].

Micro-magnetic resonance imaging (MRI)-Cardiac micro-MRI was performed under isoflurane anesthesia 8 weeks after sham operation or TAC using a Bruker Biospec, 9.4 Tesla (horizontal bore, 20 cm), small animal MRI scanner (Bruker BioSpin, Ettlingen, Germany) equipped with an actively shielded gradient insert (1200 mT/m) and a 3.5-cm quadrature coil (Bruker Biospin). For localization purposes, 2-dimensional retrospectively triggered (Intragate, Bruker BioSpin) pseudo short-axis and long-axis T1-weighted images were recorded (fast low angle shot, repetition time 6 ms, echo time 1.59 ms, flip angle 15°, matrix 192 x 192, field of view 30 x 30 mm, slice thickness 500 µm; navigator settings: size 76, 1 ms, flip angle 2.5°). A stack of short-axis images (inter-slice distance 1 mm) was then recorded from covering the full heart. Data were reconstructed using Paravision 5.1 (Bruker) by zerofilling to a matrix of 320 x 320 (in-plane resolution 94 x 94 µm) and verifying retrospective triggering accuracy before final reconstruction to 15 frames (using 70% of the respiration signal). Volumes including papillary muscles were derived from manual delineation in ImageJ (http://imageJ.nih.gov/ij; NIH, USA). Myocardial mass was derived assuming a density of 1.053 g/µl.

Statistical analysis-All data are expressed as means ± standard error of the means (SEM). Parameters between four groups were compared by one-way analysis of variance followed by Bonferroni multiple comparisons post-test for comparing sham groups, TAC groups, and sham versus respective TAC groups using GraphPad Instat (GraphPad Software, San Diego, USA). When indicated, a logarithmic transformation or a square root transformation or a non-parametric test was performed. Parameters between two groups were compared using Student's t test. When indicated, a logarithmic transformation, a square root transformation, or a non-parametric Mann-Whitney test was performed. The assumption of Gaussian distribution was tested using the method Kolmogorov and Smirnov. Kaplan-Meier survival curves were analyzed by log-rank test using Prism4 (GraphPad Software). A two-sided p-value of less than 0.05 was considered statistically significant.

SUPPLEMENTAL REFERENCES

1. Jacobs, F, Snoeys, J, Feng, Y, Van Craeyveld, E, Lievens, J, Armentano, D*, et al.* (2008). Direct comparison of hepatocyte-specific expression cassettes following adenoviral and nonviral hydrodynamic gene transfer. *Gene Ther* **15**: 594-603.
2. Lock, M, Alvira, M, Vandenberghe, LH, Samanta, A, Toelen, J, Debyser, Z*, et al.* (2010). Rapid, simple, and versatile manufacturing of recombinant adeno-associated viral vectors at scale. *Human gene therapy* **21**: 1259-1271.
3. Buys, ES, Raher, MJ, Blake, SL, Neilan, TG, Graveline, AR, Passeri, JJ*, et al.* (2007). Cardiomyocyte-restricted restoration of nitric oxide synthase 3 attenuates left ventricular remodeling after chronic pressure overload. *Am J Physiol Heart Circ Physiol* **293**: H620-627.
4. Hu, P, Zhang, D, Swenson, L, Chakrabarti, G, Abel, ED, and Litwin, SE (2003). Minimally invasive aortic banding in mice: effects of altered cardiomyocyte insulin signaling during pressure overload. *Am J Physiol Heart Circ Physiol* **285**: H1261-1269.
5. Weiss, JL, Frederiksen, JW, and Weisfeldt, ML (1976). Hemodynamic determinants of the time-course of fall in canine left ventricular pressure. *J Clin Invest* **58**: 751-760.
6. Jacobs, F, Van Craeyveld, E, Feng, Y, Snoeys, J, and De Geest, B (2008). Adenoviral low density lipoprotein receptor attenuates progression of atherosclerosis and decreases tissue cholesterol levels in a murine model of familial hypercholesterolemia. *Atherosclerosis* **201**: 289-297.
7. Camus, MC, Chapman, MJ, Forgez, P, and Laplaud, PM (1983). Distribution and characterization of the serum lipoproteins and apoproteins in the mouse, Mus musculus. *J Lipid Res* **24**: 1210-1228.
8. Van Veldhoven, PP, Swinnen, JV, Esquenet, M, and Verhoeven, G (1997). Lipase-based quantitation of triacylglycerols in cellular lipid extracts: requirement for presence of detergent and prior separation by thin-layer chromatography. *Lipids* **32**: 1297-1300.
9. Van Veldhoven, PP, Meyhi, E, and Mannaerts, GP (1998). Enzymatic quantitation of cholesterol esters in lipid extracts. *Anal Biochem* **258**: 152-155.
10. Arroyo, AI, Camoletto, PG, Morando, L, Sassoe-Pognetto, M, Giustetto, M, Van Veldhoven, PP*, et al.* (2014). Pharmacological reversion of sphingomyelin-induced dendritic spine anomalies in a Niemann Pick disease type A mouse model. *EMBO Mol Med* **6**: 398-413.
11. Van Veldhoven, PP, and Mannaerts, GP (1987). Inorganic and organic phosphate measurements in the nanomolar range. *Anal Biochem* **161**: 45-48.
12. Lenaerts, I, Driesen, RB, Hermida, N, Holemans, P, Heidbuchel, H, Janssens, S*, et al.* (2013). Role of nitric oxide and oxidative stress in a sheep model of persistent atrial fibrillation. *Europace : European pacing, arrhythmias, and cardiac electrophysiology : journal of the working groups on cardiac pacing, arrhythmias, and cardiac cellular electrophysiology of the European Society of Cardiology* **15**: 754-760.
13. Junqueira, LC, Bignolas, G, and Brentani, RR (1979). Picrosirius staining plus polarization microscopy, a specific method for collagen detection in tissue sections. *Histochem J* **11**: 447-455.
14. Shimizu, I, Minamino, T, Toko, H, Okada, S, Ikeda, H, Yasuda, N*, et al.* Excessive cardiac insulin signaling exacerbates systolic dysfunction induced by pressure overload in rodents. *J Clin Invest* **120**: 1506-1514.
15. Muthuramu, I, Singh, N, Amin, R, Nefyodova, E, Debasse, M, Van Horenbeeck, I*, et al.* (2015). Selective homocysteine-lowering gene transfer attenuates pressure overload-induced cardiomyopathy via reduced oxidative stress. *J Mol Med (Berl)* **93**: 609-618.
16. Nuutila, P, Maki, M, Laine, H, Knuuti, MJ, Ruotsalainen, U, Luotolahti, M*, et al.* (1995). Insulin action on heart and skeletal muscle glucose uptake in essential hypertension. *J Clin Invest* **96**: 1003-1009.